Electrochimica Acta 298 (2019) 704–708

Contents lists available at ScienceDirect

Electrochimica Acta

journal homepage: www.elsevier.com/locate/electacta

Wettability effects of thin titanium liquid/gas diffusion layers in proton exchange membrane electrolyzer cells

Yifan Li [a], Zhenye Kang [a], Xuanli Deng [b], Gaoqiang Yang [a], Shule Yu [a], Jingke Mo [a], Derrick A. Talley [a], G. Kane Jennings [b], Feng-Yuan Zhang [a, *]

[a] Department of Mechanical, Aerospace & Biomedical Engineering, UT Space Institute, University of Tennessee, Knoxville, United States
[b] Department of Chemical and Biomolecular Engineering Vanderbilt University, United States

ARTICLE INFO

Article history:
Received 18 September 2018
Received in revised form
10 December 2018
Accepted 28 December 2018
Available online 2 January 2019

Keywords:
Wettability
Self-assembled monolayer
Thin/tunable liquid/gas diffusion layers
Bubbles dynamics
Proton exchange membrane electrolyzer cells

ABSTRACT

Wettability of titanium thin/tunable liquid/gas diffusion layers (TT-LGDLs) may affect the oxygen bubble dynamics and detachment process, and impact the performance (cell voltage) in proton exchange membrane electrolyzer cells (PEMECs). In this study, a silane monolayer is applied to tune the TT-LGDL wettability for the first time. The ultra-fast and micro-scale oxygen gas bubble dynamics and the two-phase flow in the channel are studied *in situ* for hydrophobically treated and hydrophilic titanium thin/tunable LGDLs (TT-LGDLs) with a high-speed and micro-scale visualization system (HMVS). The HMVS shows that the micro oxygen bubbles occur only along the CL/TT-LGDL interfaces at the rim of pores on TT-LGDLs. Bubbles more easily coalescence to form a large one in hydrophobic TT-LGDLs. Pore-scale analysis on the single bubble evolution process shows that the detachment diameter and frequency of oxygen bubbles in the hydrophobic TT-LGDLs are much larger than those in the hydrophilic TT-LGDLs. The PEMEC performance with the hydrophobic and hydrophilic TT-LGDLs are very close under 2.0 A/cm^2, which means that the wettability has limited effect on TT-LGDLs mainly due to their thin features and unique structures with straight pores.

1. Introduction

Efficient production of hydrogen can lead to the development of a “hydrogen society” with close-to-zero emission of pollutants and limited environmental impact [1–6]. Proton exchange membrane electrolyzer cells (PEMEC) have been considered as one of the most promising energy storage/conversion devices for hydrogen production, especially when coupled with intermittent sustainable energy resources, including solar, wind, tides, etc., due to the advantages of high purity products, quick response, high working current density, and compact design [7–10]. Many researchers have focused on developing high-efficiency, low-cost, and durable PEMECs based on the design of novel materials and structures and the study of two-phase flow and bubble dynamics in PEMECs, and the effect of bubble dynamics on the performance is very attractive [11–16].

The typical PEMEC has a similar configuration of a PEM fuel cell (PEMFC), which consists of a membrane electrode assembly (MEA) sandwiched by liquid/gas diffusion layers (LGDLs), bipolar plates (BPs), and end plates. LGDLs, which are located between the catalyst layers (CLs) and BPs, have a porous structure and must meet certain requirements. During operation, the water transported from the BP flow field to the CLs is split into molecular oxygen, electrons, and protons at the anode side. Then, the produced oxygen gas should be effectively removed from the surface of the CLs to avoid blocking the water pathway. Electrons are transported from the CLs through the LGDLs and BPs to the external circuit [17]. Thus, LGDLs should transport electrons, heat, and reactants/products simultaneously with minimal losses [18–20]. In addition, the structures, materials, and properties of the anode LGDLs have a great impact on PEMEC performance, and efficient mass transport of liquid water and oxygen gas is critical for stable PEMEC operation. Despite its importance, however, correlation between LGDL properties, PEMEC performance, and the oxygen bubble dynamics has not been extensively studied.

Previous researchers have found that an optimum amount of coating by a hydrophobic agent on GDLs, such as polytetrafluoroethylene (PTFE) or fluorinated ethylene propylene (FEP), have

* Corresponding author.
E-mail address: fzhang@utk.edu (F.-Y. Zhang).

https://doi.org/10.1016/j.electacta.2018.12.162
0013-4686/

important impacts on two-phase transport and PEMFC performance by facilitating liquid water removal [21–30]. Zhang et al. in-situ visualized the liquid water droplet formation, growth, and detachment on GDLs and catalyst layers, and revealed the liquid water removal mechanism in flow channels of PEMFCs [31–33]. Mortazavi et al. have investigated the effects of PTFE in GDLs on water droplet growth and detachment in the flow channels. They report that the droplet has a smaller detachment size from the GDL surface with the more hydrophobic PTFE coating due to its effect on the capillary pressure and surface roughness [34,35]. Koresawa et al. developed a desired wettability distribution GDL by applying the hydrophobic coating locally and leaving the other regions unchanged. They found that the oxygen diffusivity with 10–20 wt% PTFE in the hydrophobic region was increased three times compared to the GDLs with a homogeneous wettability [36]. Lim et al. investigated FEP hydrophobic polymer content in a carbon paper GDL on the power performance of H_2/air PEMECs. The contact angle measurements indicate a similar level of hydrophobicity among GDLs impregnated with different amounts of FEP ranging from 10 to 40 wt% [37]. Litster et al. employed fluorescence microscopy with a novel methodology to provide new insight into the dynamic behavior and distribution of liquid water as it is transported through the gas diffusion layers in PEMECs. The experimental observations led to the postulation of the primary mechanism for liquid water transport in hydrophobic GDLs [38]. Pasaogullari et al. examined the governing physics of liquid water transport in hydrophobic GDLs. They observed that capillary transport is the dominant transport process to remove water from flooded GDLs [39]. Very few studies have investigated the effects of GDL wettability in unitized regenerative fuel cells (URFCs) and PEMECs. Ioroi et al. said that PTFE in hydrogen electrode GDLs has nearly no effect on cell performance in both FC and EC modes, but the PTFE in oxygen electrode GDLs had a negative impact on URFC performance in EC mode and improved performance in FC mode especially under fully wet working conditions [40]. But on the contrary, Hwang et al. found that the PTFE coating has no effect on URFC performance under the EC mode. They also said that the PTFE coating in titanium GDLs can improve the URFC performance under both dry and wet conditions in FC mode, while it will negatively impact the performance under mid-range humidity [41–43]. Kang et al. developed a novel thin/tunable gas diffusion electrode, and achieved a very good performance. More significantly, the Pt mass activity for hydrogen evolution reaction has also been greatly increased [44].

The treatment of GDLs in PEMFCs have been fully investigated; however, research focused on ultrathin LGDL hydrophobic treatment in PEMECs has never been reported. The relations between the GDL wettability, gas bubble dynamics, and PEMEC performance are still unknown. Therefore, thorough analysis is needed for better understanding of how the wettability changes the bubble dynamics and impacts PEMEC performance. In this study, the Ti based thin/tunable LGDLs (TT-LGDLs) are hydrophobically treated by a monolayer film from n-octadecyltrichlorosilane in one simple step. Both the fresh TT-LGDLs and the hydrophobic TT-LGDLs are characterized both *in-situ* and *ex-situ*. The wettability of the two TT-LGDLs are measured by water contact angle. By taking advantages of the in-house built high-speed and micro-scale visualization system (HMVS), novel TT-LGDLs and the transparent PEMECs, the oxygen bubble dynamics, and the two-phase flow phenomenon in an operating PEMEC are captured *in-situ*. The PEMEC performance between the two TT-LGDLs is also tested, and the relation between the performance and wettability is analyzed. The results obtained in this study point out the direction for optimized LGDL wettability and the new method for investigation of the bubble dynamics in PEMECs.

2. Experimental details

A TT-LGDL was used in this study, and was experimental measured with a microscope, the thickness is 25 μm, the porosity is 55%, a circular pore shape, and a pore diameter of ~300 μm. In our previous studies, the TT-LGDLs achieved excellent PEMEC performance [20,45–47] and their straight-through pores allow the *in-situ* visualization of oxygen bubble dynamics. In order to hydrophobically treat the TT-LGDLs, the fresh sample was rinsed in ethanol, and thoroughly dried, and then placed in a 1 mM solution of octadecyltrichlorosilane in toluene for 1 h. The reason we selected this molecule is because the trichlorosilane head group reacts well with many oxide surfaces, and the molecule has a long chain for good stability and excellent hydrophobicity. The thickness of this film was estimated to be about 2.5 nm, based on the structure of the monolayer, the number of carbons and associated bond lengths [48,49]. The surface roughness should be negligible for the film itself, as n-alkyl trichlorosilanes are known to form dense monolayers on titanium [50]. Fig. 1 schematically shows the structure of the monolayer as prepared from n-octadecyltrichlorosilane ($CH_3(CH_2)_{17}SiCl_3$; $C_{18}SiCl_3$). As established by Mani et al., the principal binding of the molecule to the oxide surface of titanium is through Si–O–Ti bonds with minimal Si–O–Si cross-linking, leading to a densely packed hydrocarbon film.

The specific, designed transparent cell, as shown in Fig. 2, was used to test the PEMEC performance and to perform visualization of micro bubble dynamics and two-phase transport. Different from

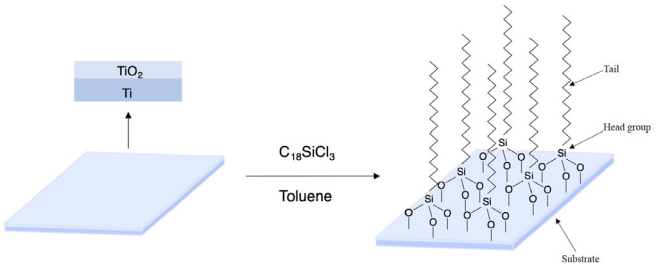

Fig. 1. Schematic for the formation of a monolayer film from n-octadecyl trichlorosilane onto titanium.

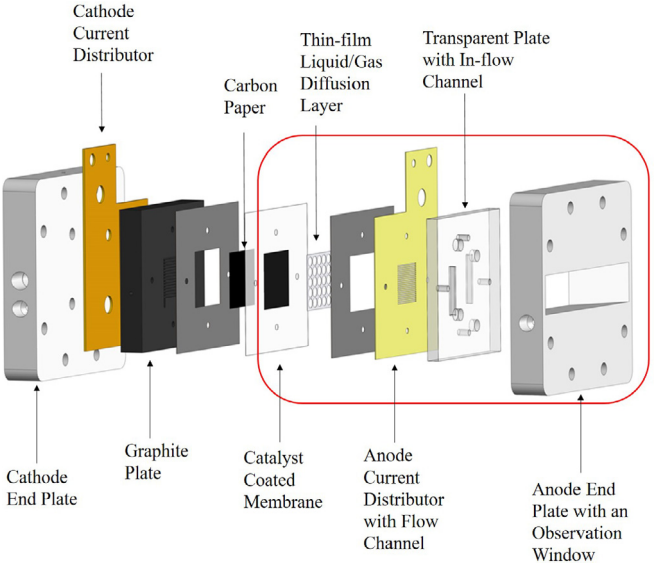

Fig. 2. Schematic of the transparent PEMEC.

the typical PEMECs, the anode transparent PEMEC as shown in the red box, has an end plate with a window on the center, a transparent plate, a current distributor with flow channels, and TT-LGDLs, which help to allow optical access to the CL surface. The transparent plate with flow ports and in-flow channels is used to transport reactants from the cell inlet to the flow channels, and products from the flow channels to the outlet of the cell. The current distributor is a 500 mm thick titanium plate with chemically etched parallel micro flow channels of 1 mm in channel width that penetrated the entire thickness. TT-LGDLs with a thickness of only 25 μm are used. Since the oxygen bubble dynamics occur at the micro-scale at a super high-speed, the phenomena cannot be effectively captured by the normal microscopes or cameras. Therefore, besides the transparent cell and TT-LGDLs, the HMVS with a long-working distance is another critical part of the whole system. The HMVS consists of a high-speed camera (Phantom V711) coupled with an in-house built optical lens system featured by its long working distance (>70 mm) and a high resolution (<5 μm). The movie is captured under a frame rate of 3000 fps (frame per second), and the bubble detachment time within TT-LGDL were calculated based on the frame rate.

Commercial CCM (Nafion 115 Electrolyzer CCM from FuelCellsEtc with 3.0 mg/cm^2 IrRuOx at anode and 3.0 mg/cm^2 PtB at cathode) is employed, and the active area of the CCM is 5 cm^2. Carbon paper (Toray 090 from FuelCellStore) with a 280 μm thickness and 78% porosity is used as a cathode LGDL. Graphite plates with a parallel flow channel are used as cathode BP. The transparent cell is connected to the Potentiostat SP-300 (Bio-Logic) system that was equipped with a 10 A/5 V booster. A liquid pump (KNF Neuberger) is used to circulate deionized water at a flow rate of 20 mL/min to the anode.

The sessile drop method is used to measure the contact angle. The measured TT-LGDLs are placed on the top of a plastic substrate and a 2 μL droplet of distilled water is dropped from the tip to the surface of the TT-LGDLs, including the fresh and hydrophobic TT-LGDLs. The image of the droplet is collected and the contact angle is measured in this image by the software. Three measurements at different spots are obtained for each sample and an average is calculated and reported as the contact angle.

3. Results and discussion

The treated TT-LGDL has a much higher contact angle (127°) than the untreated one (86°) due to the presence of the dense, low-energy methyl-terminated monolayer that effectively screens the interaction between water and titanium, as shown in Fig. 3. These results show that the monolayer treatment can significantly change the wettability of the TT-LGDLs. As a control, we also prepared silane monolayers on non-porous titanium foils. As with the LGDLs, the presence of the monolayer increases the water contact angle—in this case, from 68° to 110°. The value of 110° is consistent with that of a smooth and dense methyl surface and is similar to the values reported by Mani et al. for silane monolayers on titanium. The water contact angles on the LGDL are elevated from those on the Ti foil due to the imparted roughness of the LGDL, which may stabilize air under the water drop and at the three-phase contact line.

Both the hydrophobic and hydrophilic TT-LGDLs were evaluated in the transparent PEMEC at 80 °C. Because the transparent plate is made of plastic and the current distributor is relative thin, which may cause a non-uniform pressure distribution along the surface and thus a larger ohmic loss than that of the conventional PEMECs. The high frequency resistance (HFR) values under a frequency of 5000 Hz are about 0.24 Ω*cm^2 for the treated TT-LGDL, and about 0.22 Ω*cm^2 for the non-treated one, respectively. The result shows

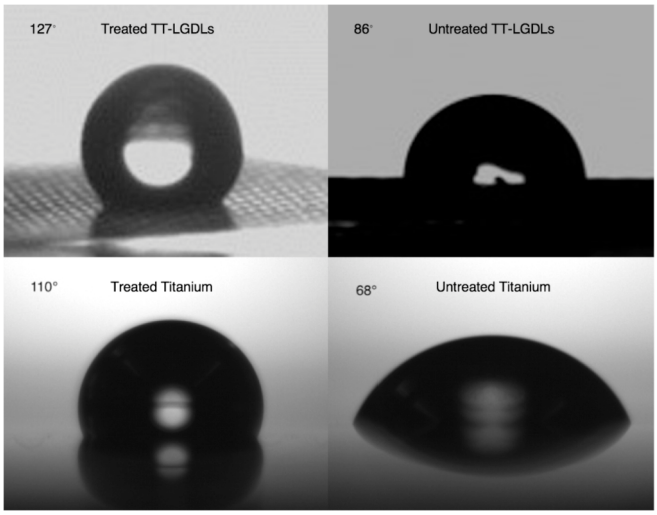

Fig. 3. Contact angle measurements for (top) treated and untreated TT LGDLs and (bottom) treated and untreated Ti foil.

that the SAM can lead to a very limited changes about ohmic losses. The performance of the PEMECs is characterized by the IR-free voltage, which is derived based on polarization curves and high frequency resistance (HFR), as shown in Fig. 4. The lower voltage at a given current density indicates better PEMEC performance. As is shown in Fig. 4, the performance of the hydrophobic TT-LGDLs is a little bit worse than the hydrophilic one. At the low current density range (<0.1 A/cm^2), the polarization curves are mainly due to the open circuit voltage (OCV) and activation overpotential. From Fig. 4, the hydrophobic and the hydrophilic TT-LGDLs have a similar voltage, which means the wettability of the TT-LGDLs has no impact on activation loss. At 2.0 A/cm^2, the required cell voltage increased from 1.620 V for the hydrophilic TT-LGDLs to about 1.624 V for the hydrophobic TT-LGDLs which indicates that the wettability of the TT-LGDLs has very limited impact on PEMEC performance. With a 2.5 nm thickness, it can be assumed that the monolayer film will not affect the electrical conductivity of the TT-LGDLs as long as the temperature is in a range from 20 °C to 80 °C, and also the electrical contact resistance between TT-LGDLs/CLs and TT-LGDLs/BPs

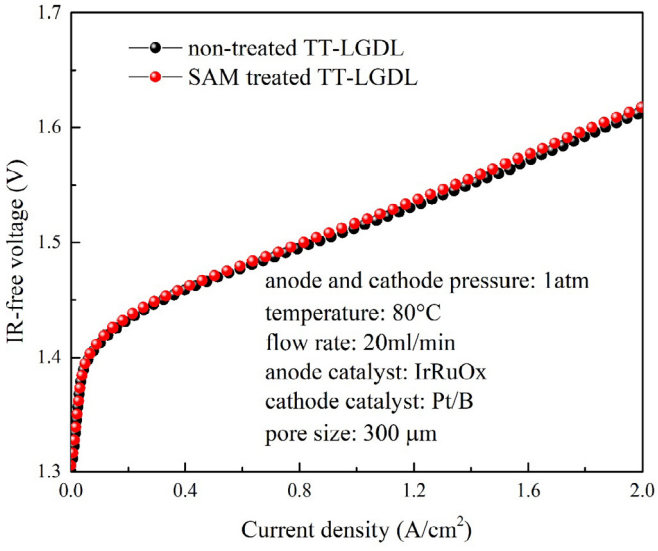

Fig. 4. The polarization curves of the hydrophobic and hydrophilic TT-LGDLs.

[18,51]. In addition, the monolayer does not change the pore morphologies of the TT-LGDLs, which will not influence the activation loss. The monolayer on TT-LGDLs will only change the wettability of the Ti TT-LGDLs from 86° to 127°, which may have some effects on transport loss in the PEMEC. Therefore, the influence of the monolayer on bubble dynamics, and two-phase transport will be investigated.

Fig. 5 shows the two-phase flow phenomena comparison at channel-scale, Fig. 5(A) and (B) are bubble dynamics at 0.2 A/cm^2, 80 °C, Fig. 5(C) and (D) are bubble dynamics at 1.4 A/cm^2, 80 °C. It can be found that the most oxygen bubbles in the channel with the hydrophobic TT-LGDLs are much larger (as shown in Fig. 5(A) and (C)) than the bubble sizes with the hydrophilic TT-LGDLs (as shown in Fig. 5(B) and (D)). After the bubble detachment, some bubbles will collide and then merge with each other to form a large bubble. Under the same operating conditions, the larger bubbles with higher surface area and large volume have higher probability to merge with other bubbles; therefore, the hydrophobic TT-LGDLs with larger detached oxygen bubbles can lead to larger bubble sizes within the flow channel than those observed for the hydrophilic TT-LGDLs. These phenomena are very common in the whole channel in the PEMECs.

Fig. 6 shows a sequence of images of pore-scale bubble generation and movement, with photographs of an oxygen gas bubble appearance, growth, and finally, detachment. The bubble dynamics are different for different locations, due to the different force balance in the water flow. Therefore, the oxygen bubbles we chose with the two different TT-LGDLs are nearly at the same location in the cell and pore. Fig. 6(A)–(D) and (E) to (H) show the oxygen bubble generation and growth with hydrophilic and hydrophobic TT-LGDLs at 0.2 A/cm^2 and 80 °C, respectively. Fig. 6 shows that the oxygen bubbles only generate at the rim of the TT-LGDL pores,

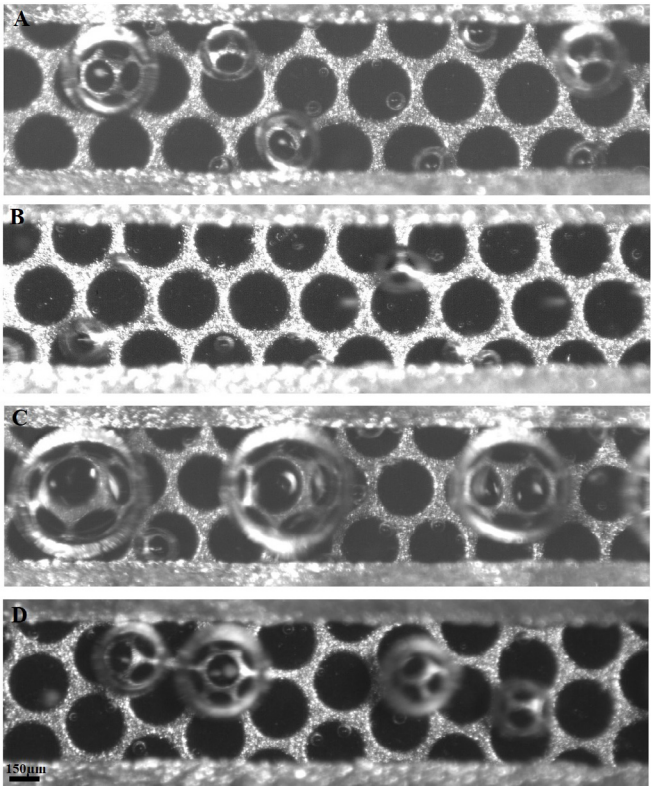

Fig. 5. The visualization results at channel scale: (A) hydrophobic TT-LGDLs and (B) hydrophilic TT-LGDLs at 0.2 A/cm^2 and 80°; (C) hydrophobic TT-LGDLs and (D) hydrophilic TT-LGDLs at 1.4 A/cm^2 and 80 °C.

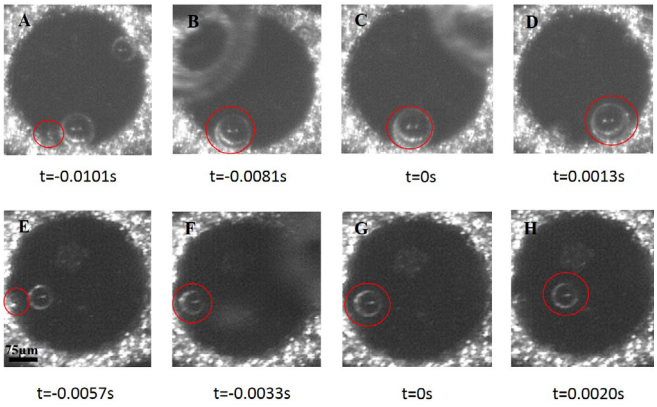

Fig. 6. The visualization results of pore scale (A) to (D) hydrophobic TT-LGDLs and (E) to (H) hydrophilic TT-LGDLs at 0.2 A/cm^2 and 80 °C.

which is the same phenomena as compared to our previous research and can be attributed to the large in-plane electrical resistance of the CLs [52]. The oxygen bubble will appear at the rim of the pore, then it will grow and detach within a couple of milliseconds. Fig. 6 (C) and (G) show the bubble detachment from the surface of the two TT-LGDLs. The bubble detachment diameter for the hydrophilic TT-LGDLs (about 57 μm) is smaller than the hydrophobic one (about 84 μm). Also, the bubble detachment time for the hydrophilic TT-LGDLs (about 0.0057 s) is shorter than the hydrophobic one (about 0.0101 s). The reason is that bubbles are prone to attach on the hydrophobic surface of the treated TT-LGDL (contact angle > 90°), and easily to detach from a hydrophilic TT-LGDL (contact angle < 90°). Moreover, this successive bubble behavior occurs in a repetitive manner at the same points. Considering the PEMEC performance shown in Fig. 4, we conclude that the hydrophobic treatment on TT-LGDLs has a negative impact on bubble detachment, which could increase the transport loss in the PEMEC, but this result has limited effect on PEMEC performance under 2.0 A/cm^2. Because the advantages of the TT-LGDLs, such as planar surfaces, straight-through pores, and small thickness, the transport losses will be limited. Although the monolayer film will increase the bubble detachment diameter and bubble size in the channels, the increase of transport loss due to these reasons is very small compared with the total loss in the PEMEC. Considering that the monolayer film has no effect on ohmic and activation losses, it will not have significant influence on PEMEC performance, especially under 2.0 A/cm^2. We expect that the performance of the hydrophobic TT-LGDLs will be degraded under much higher current densities due to the large bubble detachment, which may cause additional two-phase transport losses in a PEMEC.

4. Summary

In this study, the hydrophilic titanium TT-LGDLs are treated by a silane monolayer to change their wettabilities for the first time. The micro-scale and ultra-fast oxygen bubble dynamics are *in-situ* visualized in a novel designed transparent PEMEC with a HMVS. The results show that the oxygen bubble detachment diameter and frequency of the hydrophobic TT-LGDLs are much larger than ones with the hydrophilic TT-LGDLs, and the bubble size in the channel scale with the hydrophobic TT-LGDLs is much larger than the one with the hydrophilic TT-LGDLs as well. The PEMEC performance with the hydrophobic and hydrophilic TT-LGDLs are very close. The advantages of the TT-LGDLs, such as planar surface, straight-through pores, and small thickness result in very limited difference of the transport losses between the hydrophobic and

hydrophilic TT-LGDLs. The increase of the transport loss due to these reasons is very small compared with the total loss in the PEMEC, especially under 2.0 A/cm^2. We expect that the performance of the hydrophobic TT-LGDLs will be degraded under much higher current densities, due to the large bubble detachment which may cause additional two-phase transport losses in a PEMEC.

Acknowledgment

The authors greatly appreciate the support from U.S. Department of Energy's National Energy Technology Laboratory under Award DE-FE0011585, and National Renewable Energy Laboratory under Award DE-AC36-08GO28308. This research was partially conducted at the Center for Nanophase Materials Sciences, which is a DOE Office of Science User Facility. The authors also wish to express their appreciation to Dr. Scott Retterer, Dr. David Cullen, Dr Lee Leonard, Dr. Jackie Johnson, Dr. Bo Han, William Barnhill, Stuart Steen, Dale Hensley, Daryl Briggs, Alexander Terekhov, Douglas Warnberg, and Kate Lansford for their help.

References

[1] J.A. Turner, Sustainable hydrogen production, Science 305 (5686) (2004) 972–974.
[2] H. Ito, et al., Experimental study on porous current collectors of PEM electrolyzers, Int. J. Hydrogen Energy 37 (9) (2012) 7418–7428.
[3] T. Yoshida, K. Kojima, Toyota MIRAI fuel cell vehicle and progress toward a future hydrogen society, Electrochem. Soc. Interface 24 (2) (2015) 45–49.
[4] J.R. Rostrup-Nielsen, Making fuels from biomass, Science 308 (5727) (2005) 1421–1422.
[5] K.E. Ayers, et al., Research advances towards low cost, high efficiency PEM electrolysis, ECS Trans. 33 (1) (2010) 3–15.
[6] J.H. Lin, et al., Effect of various hydrophobic concentrations and base weights of gas diffusion layer for proton exchange membrane fuel cells, Fuel Cell. 10 (1) (2010) 118–123.
[7] Z. Kang, et al., Investigation of thin/well-tunable liquid/gas diffusion layers exhibiting superior multifunctional performance in low-temperature electrolytic water splitting, Energy Environ. Sci. 10 (1) (2017) 166–175.
[8] G. Yang, et al., Additive manufactured bipolar plate for high-efficiency hydrogen production in proton exchange membrane electrolyzer cells, Int. J. Hydrogen Energy 42 (21) (2017) 14734–14740.
[9] J. Mo, et al., Additive manufacturing of liquid/gas diffusion layers for low-cost and high-efficiency hydrogen production, Int. J. Hydrogen Energy 41 (4) (2016) 3128–3135.
[10] J. Mo, et al., Visualization on rapid and micro-scale dynamics of oxygen bubble evolution in PEMECs, in: Nano/micro Engineered and Molecular Systems (NEMS), IEEE 12th International Conference on. 2017. IEEE, 2017.
[11] C. Lamy, et al., Clean hydrogen generation through the electrocatalytic oxidation of ethanol in a Proton Exchange Membrane Electrolysis Cell (PEMEC): effect of the nature and structure of the catalytic anode, J. Power Sources 245 (2014) 927–936.
[12] C. Lamy, et al., Kinetics analysis of the electrocatalytic oxidation of methanol inside a DMFC working as a PEM electrolysis cell (PEMEC) to generate clean hydrogen, Electrochim. Acta 177 (2015) 352–358.
[13] J. Mo, et al., Investigation of titanium felt transport parameters for energy storage and hydrogen/oxygen production, in: 13th International Energy Conversion Engineering Conference, 2015.
[14] J. Mo, S. Steen, F.-Y. Zhang, High-speed and micro-scale measurements of flow and reaction dynamics for sustainable energy storage, in: 13th International Energy Conversion Engineering Conference, 2015.
[15] J. Mo, et al., Discovery of true electrochemical reactions for ultrahigh catalyst mass activity in water splitting, Sci. Adva. 2 (11) (2016) e1600690.
[16] T.J. Toops, et al., Evaluation of Nitrided Titanium separator plates for proton exchange membrane electrolyzer cells, J. Power Sources 272 (2014) 954–960. **2014**.
[17] J. Mo, et al., Electrochemical investigation of stainless steel corrosion in a proton exchange membrane electrolyzer cell, Int. J. Hydrogen Energy 40 (36) (2015) 12506–12511.
[18] B. Han, et al., Effects of membrane electrode assembly properties on two-phase transport and performance in proton exchange membrane electrolyzer cells, Electrochim. Acta 188 (2016) 317–326.
[19] B. Han, et al., Modeling of two-phase transport in proton exchange membrane electrolyzer cells for hydrogen energy, Int. J. Hydrogen Energy 42 (7) (2017) 4478–4489.
[20] Z. Kang, et al., Thin film surface modifications of thin/tunable liquid/gas diffusion layers for high-efficiency proton exchange membrane electrolyzer cells, Appl. Energy 206 (2017) 983–990.
[21] R. Omrani, B. Shabani, Gas diffusion layer modifications and treatments for improving the performance of proton exchange membrane fuel cells and electrolysers: a review, Int. J. Hydrogen Energy (2017).
[22] F.-Y. Zhang, S.G. Advani, A.K. Prasad, Performance of a metallic gas diffusion layer for PEM fuel cells, J. Power Sources 176 (1) (2008) 293–298.
[23] F.-Y. Zhang, A.K. Prasad, S.G. Advani, Investigation of a copper etching technique to fabricate metallic gas diffusion media, J. Micromech. Microeng. 16 (11) (2006) N23.
[24] S. Matar, H. Liu, Effect of cathode catalyst layer thickness on methanol crossover in a DMFC, Electrochim. Acta 56 (1) (2010) 600–606.
[25] L. You, H. Liu, A parametric study of the cathode catalyst layer of PEM fuel cells using a pseudo-homogeneous model, Int. J. Hydrogen Energy 26 (9) (2001) 991–999.
[26] D. Natarajan, T. Van Nguyen, Three-dimensional effects of liquid water flooding in the cathode of a PEM fuel cell, J. Power Sources 115 (1) (2003) 66–80.
[27] P. Stampino, et al., Effect of different hydrophobic agents onto the surface of gas diffusion layers for PEM-FC, Chem. Eng. 32 (2013).
[28] Y.R. Thomas, et al., New method for super hydrophobic treatment of gas diffusion layers for proton exchange membrane fuel cells using electrochemical reduction of diazonium salts, ACS Appl. Mater. Interfaces 7 (27) (2015) 15068–15077.
[29] T.-J. Ko, et al., High performance gas diffusion layer with hydrophobic nanolayer under a supersaturated operation condition for fuel cells, ACS Appl. Mater. Interfaces 7 (9) (2015) 5506–5513.
[30] S. Kim, et al., Effects of hydrophobic agent content in macro-porous substrates on the fracture behavior of the gas diffusion layer for proton exchange membrane fuel cells, J. Power Sources 270 (2014) 342–348.
[31] F.Y. Zhang, et al., In situ characterization of the catalyst layer in a polymer electrolyte membrane fuel cell, J. Electrochem. Soc. 154 (11) (2007) B1152–B1157.
[32] F.Y. Zhang, X.G. Yang, C.Y. Wang, Liquid water removal from a polymer electrolyte fuel cell, J. Electrochem. Soc. 153 (2) (2006) A225–A232.
[33] X.G. Yang, et al., Visualization of liquid water transport in a PEFC, Electrochem. Solid State Lett. 7 (11) (2004) A408–A411.
[34] M. Mortazavi, K. Tajiri, Effect of the PTFE content in the gas diffusion layer on water transport in polymer electrolyte fuel cells (PEFCs), J. Power Sources 245 (2014) 236–244.
[35] M. Mortazavi, K. Tajiri, Liquid water breakthrough pressure through gas diffusion layer of proton exchange membrane fuel cell, Int. J. Hydrogen Energy 39 (17) (2014) 9409–9419.
[36] R. Koresawa, Y. Utaka, Improvement of oxygen diffusion characteristic in gas diffusion layer with planar-distributed wettability for polymer electrolyte fuel cell, J. Power Sources 271 (2014) 16–24.
[37] C. Lim, C. Wang, Effects of hydrophobic polymer content in GDL on power performance of a PEM fuel cell, Electrochim. Acta 49 (24) (2004) 4149–4156.
[38] S. Litster, D. Sinton, N. Djilali, Ex situ visualization of liquid water transport in PEM fuel cell gas diffusion layers, J. Power Sources 154 (1) (2006) 95–105.
[39] U. Pasaogullari, C. Wang, Liquid water transport in gas diffusion layer of polymer electrolyte fuel cells, J. Electrochem. Soc. 151 (3) (2004) A399–A406.
[40] T. Ioroi, et al., Influence of PTFE coating on gas diffusion backing for unitized regenerative polymer electrolyte fuel cells, J. Power Sources 124 (2) (2003) 385–389.
[41] C.-M. Hwang, et al., Effect of PTFE contents in the gas diffusion layers of polymer electrolyte-based unitized reversible fuel cells, J. Int. Counc. Electr. Eng. 2 (2) (2012) 171–177.
[42] C.M. Hwang, et al., Influence of properties of gas diffusion layers on the performance of polymer electrolyte-based unitized reversible fuel cells, Int. J. Hydrogen Energy 36 (2) (2011) 1740–1753.
[43] C. Hwang, et al., Effect of through-plane polytetrafluoroethylene distribution in a gas diffusion layer on a polymer electrolyte unitized reversible fuel cell, ECS Transactions 58 (1) (2013) 1059–1068.
[44] Z. Kang, et al., Novel thin/tunable gas diffusion electrodes with ultra-low catalyst loading for hydrogen evolution reactions in proton exchange membrane electrolyzer cells, Nano Energy (2018).
[45] J. Mo, et al., Thin liquid/gas diffusion layers for high-efficiency hydrogen production from water splitting, Appl. Energy 177 (2016) 817–822.
[46] Z. Kang, et al., Investigation of novel thin LGDLs for high-efficiency hydrogen/oxygen generation and energy storage, in: 15th International Energy Conversion Engineering Conference, 2017.
[47] Y. Li, et al., In-situ investigation of bubble dynamics and two-phase flow in proton exchange membrane electrolyzer cells, Int. J. Hydrogen Energy (2018).
[48] O. Acton, et al., Spin-cast and patterned organophosphonate self-assembled monolayer dielectrics on metal-oxide-activated Si, Adv. Mater. 23 (16) (2011) 1899–1902.
[49] M. Halik, et al., Low-voltage organic transistors with an amorphous molecular gate dielectric, Nature 431 (7011) (2004) 963.
[50] G. Mani, et al., Stability of self-assembled monolayers on titanium and gold, Langmuir 24 (13) (2008) 6774–6784.
[51] G. Yang, et al., Fully printed and integrated electrolyzer cells with additive manufacturing for high-efficiency water splitting, Appl. Energy 215 (2018) 202–210.
[52] Z. Kang, et al., Performance modeling and current mapping of proton exchange membrane electrolyzer cells with novel thin/tunable liquid/gas diffusion layers, Electrochim. Acta 255 (2017) 405–416.